

Ab initio Electronic Structure Calculations and Photoelectron Spectroscopies

The knowledge of the atomic and electronic structures of a solid is fundamental for understanding its physical and chemical properties. Therefore, the electronic structure of solids has been a subject of intensive theoretical and experimental research ever since the quantum mechanics was formulated. Before mid-1980's, optical absorption and reflection and photoemission experiments using laboratory lamps were conducted to study the electronic structure of a solid. In the past two decades, however, synchrotron radiation has become an essential part of the human research tool kit because of its intense, tunable, polarized beams. Synchrotron radiation has contributed to a wide range of research, including materials and surface science, chemistry and structural and molecular biology. In the field of material science, in particular, a range of experimental techniques and spectroscopies using synchrotron radiation sources have been developed and become powerful probes of the atomic and electronic structures of materials. These developments are closely matched by advanced *ab initio* electronic structure calculations which can predict the properties of many complex materials with high precision, including structural, electrical and magnetic properties as well as the electronic structure. In this article, examples are given to illustrate how synchrotron radiation based photoelectron spectroscopies with the aid of *ab initio* electronic structure calculations can be used to obtain detailed information about the electronic structure of solid materials.

The first example is a binary intermetallic compound PtGa₂. These binary intermetallic compounds crystallize in the cubic fluorite (CaF₂) structure and exhibit many unique properties. For example, they show a striking variety of colors, ranging from purple (AuAl₂) to copper (PtIn₂) to gold (PtGa₂). Many of them also become superconducting at low temperatures. Therefore, these intermetallics have received a great deal of attention in the past fifteen years.

Angled resolved photoemission spectrum (ARPES) measurements on the (111) face of a PtGa₂ single crystal were performed recently using synchrotron radiation with photon energies in the range of 80 to 220 eV, in order to probe its valence (occupied) energy bands. In the meantime, soft X-ray absorption spectra of PtGa₂ were also measured to study its conduction (unoccupied) energy bands. Figure 1 shows a set of normal-emission photoemission spectra from PtGa₂. Clearly, there are pronounced peaks in the photoemission spectra especially between binding energies of 2 and 8 eV. Furthermore, the energy position of these features changes with varying incident photon energy. The energy positions of the features as a function of incident photon energy contain information about the electron crystal momentum inside the crystal of PtGa₂. Within a direct-transition model and the free-electron conduction-band approximation, for example, one can derive the valence band structure (i.e., the quasi-particle binding energy versus crystal momentum dispersion relation) of PtGa₂ from the ARPES. Within these assumptions, the normal component of the photoemitted electron momentum inside the crystal is given by

$$k_{\perp}^2 = \frac{2m}{\hbar} \left[\frac{m^*}{m} (E_k + V_0) - E_k \sin^2 \theta \right]$$

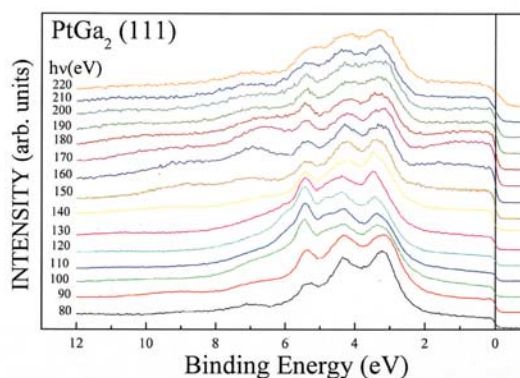


Fig. 1: Angle-resolved photoemission spectra taken at normal emission from the (111) face of PtGa₂ in the photon energy range 80 to 220 eV.

where E_k is the kinetic energy of the photoelectron in vacuum, θ is the polar angle of emission with respect to the sample normal, V_0 is the inner potential, and m^* is the effective mass of the photoelectron. The derived valence energy bands of PtGa₂ along the $L-\Gamma-L$ line in the fcc Brillouin zone are displayed in Fig. 2. Also shown in Fig. 2 are the theoretical energy bands from an ab initio calculation. The calculation was based on first-principles density functional theory with the local density approximation and was carried out using the state of the art full-potential linearized augmented wave (FLAPW) method with the spin-orbit coupling included. Clearly, there is a good quantitative agreement between the theoretical and experimentally derived energy bands. However, such a good agreement was not achieved in previous theoretical studies which used the non-selfconsistent muffin-tin potential and/or neglected the spin-orbit coupling. Pt and Au are heavy elements and the relativistic effects such as spin-orbit coupling are important and cannot be ignored. The electronic structure of PtGa₂ as shown in Fig. 2 is similar to that of fcc Au. This explains why PtGa₂ exhibits a golden color.

Another example is an intermetallic compound Ni₃In. These intermetallic compounds Ni₃Al, Ni₃Ga and Ni₃In exhibit many interesting mechanical, electronic and magnetic properties. For example, Ni₃Al displays unique high-temperature mechanical properties that have

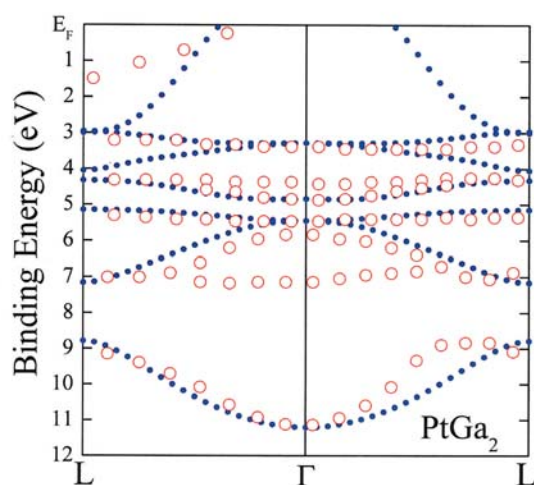


Fig. 2: Band structure of PtGa₂ along the $L-\Gamma-L$ line in the fcc Brillouin zone. Blue circles are bands derived from the ARPES data, and red dots are theoretical band structure.

possible uses in, e.g., hydroturbines and cutting tools. Furthermore, Ni₃Al shows a weak itinerant ferromagnetism with $T_c = 41.5$ K, while Ni₃Ga is an exchange-enhanced paramagnetic metal. The unique properties of these intermetallic compounds are due, in part, to the nature of their atomic/crystal and electronic structures. The electronic structure of Ni₃Al and Ni₃Ga have been extensively studied experimentally and theoretically. Both Ni₃Al and Ni₃Ga crystallize in the simple cubic Cu₃Au ($L1_2$) structure. On the other hand, the crystal structure of Ni₃In is still not clear. Some structural measurements before 1960 suggested that Ni₃In has the so-called (hexagonal) DO_{19} structure isotypic with Ni₃Sn. However, it was recently reported that Ni₃In also forms the $L1_2$ structure. However, recently measured Ni K - and $L_{2,3}$ -edge XAS spectra from Ni₃In are not in good agreement with the corresponding theoretical XAS spectra calculated assuming the $L1_2$ structure. Further, the Ni $L_{2,3}$ -edge XAS spectrum calculated using the DO_{19} structure resulted in worse agreement with experiments. The room-temperature magnetization measurements indicate that Ni₃In is nonmagnetic.

Therefore, a systematic theoretical study of the structural stability, mechanical and magnetic properties as well as the electronic structure of Ni₃In has been carried out. Again, the highly accurate FLAPW method was used and the theoretical calculations were based on the first-principles density-functional theory with the generalized gradient approximation (GGA). Like Ni₃Al, the ground state of Ni₃In is found to be the ferromagnetic $L1_2$ structure. However, unlike Ni₃Al, the tetragonal DO_{22} structure of Ni₃In is found to be nonmagnetic with the total energy being just above that of the ferromagnetic $L1_2$ but below the nonmagnetic $L1_2$ state. Thus, the theoretical calculations predict that Ni₃In would have the ferromagnetic $L1_2$ structure at low temperatures but transform to the non-magnetic tetragonal DO_{22} structure as the temperature is increased to room temperature. This prediction thus resolves the conflicts between the experiments and previous calculations, as is demonstrated below by comparing the calculated electronic structure with the X-ray photoemission experiments and XAS measurements.

Near-edge structures in X-ray absorption spectra measure the element-specific local

electronic structure and hence probe the local atomic structure around the absorbing atoms in the solid as well. The XAS arises from transitions from the core levels to the unoccupied states above the Fermi level. In the one-particle and dipole approximations, the probability (W) of the transition from a core level of angular momentum L to final unoccupied states is, according to Fermi's golden rule, given by

$$W_L \propto \left\{ |M_{L+1}|^2 N_{L+1} + |M_{L-1}|^2 N_{L-1} \right\}$$

where $M_{L\pm 1}$ are the dipole matrix elements for the transition to final unoccupied states of angular momentum $L\pm 1$, respectively. $N_{L\pm 1}$ are the local ($L\pm 1$)-decomposed DOS of the absorbing atoms above the Fermi level. Since the transition matrix elements are often a smooth monotonic function of photon energy in the near edge region, XAS spectra therefore measure largely the local ($L\pm 1$)-decomposed DOS. For the K -edge, a XAS spectrum is roughly proportional to the unoccupied p -decomposed DOS, as shown in Fig. 3 where both the experimental and theoretical Ni K -edge XAS spectra from Ni_3In are displayed together with calculated Ni p -DOS. Clearly, there is a good agreement between the theory and experiments, indicating that Ni_3In is in nonmagnetic tetragonal $D0_{22}$ structure at room temperature.

Angle-integrated X-ray photoemission spectrum (XPS) and bremsstrahlung iochromat

(i.e., inverse photoemission) (BIS) spectrum from Ni_3In are displayed in Fig. 4 together with total DOS of Ni_3In in nonmagnetic tetragonal $D0_{22}$ structure. Sophisticated theories exist that allow to calculate photoemission and inverse photoemission spectra. For XPS, however, because of high energies of photoexcited electrons, multiple-scattering can be neglected and the single-scatterer final state approximation suffices. Again, transition matrix elements are often a smooth function of photon energy and generally no single transition dominates. Therefore, XPS spectra can be taken as being essentially proportional to the total valence band DOS of the solid. Likewise, BIS spectra are roughly proportional to the total conduction band DOS. Figure 4 shows that the agreement between the theoretical valence band DOS and the XPS spectrum as well as between the theoretical conduction band DOS and the BIS spectrum from Ni_3In is rather good. In particular, the calculated Ni d -dominant bandwidth of 3 eV agrees well with the XPS measurements. This clearly indicates that the electronic structure of the intermetallics Ni_3In , Ni_3In and Ni_3In Ni_3In is well described by first-principles LDA and GGA calculations if carried out using highly accurate band structure method such as the FLAPW method.

The structural, electrical and magnetic properties as well as the electronic structure of metals and their intermetallic compounds are well described by *ab initio* calculations based on

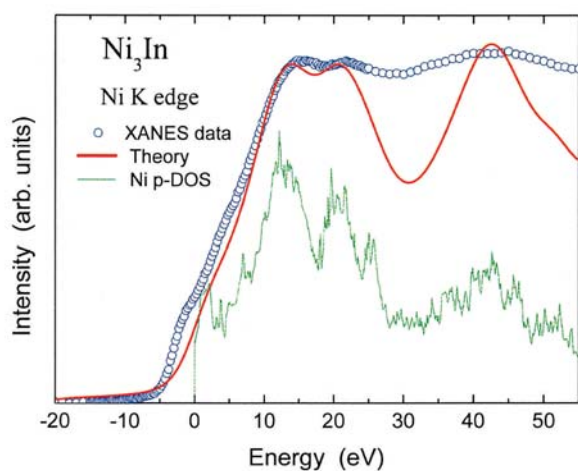


Fig. 3: The theoretical Ni K -edge XAS spectrum and also the Ni p DOS from Ni_3In in the $D0_{22}$ structure, compared with the experimental Ni K -edge XAS spectrum.

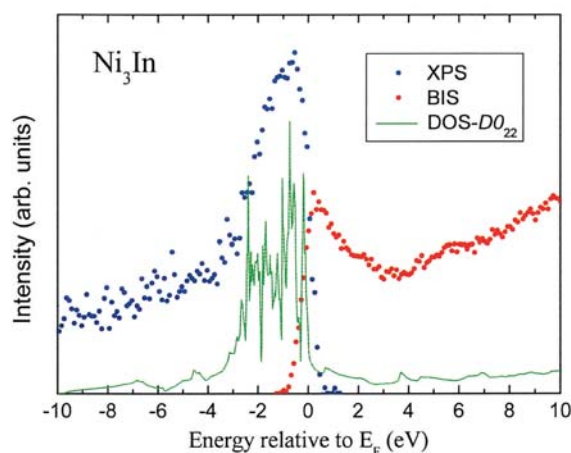


Fig. 4: Calculated density of states (DOS) of Ni_3In compared with valence-band X-ray photoemission spectra (XPS) and conduction-band bremsstrahlung iochromat spectra (BIS).

density functional theory with LDA or GGA. Indeed, with the advent of powerful computers and fast algorithms, *ab initio* calculations have contributed tremendously to scientific advances in many areas of research such as magnetism, materials and surface sciences, chemistry and even biology in the past two decades. However, LDA or GGA approximations fail miserably for many transition metal oxides where most exciting solid state phenomena observed in the past fifteen years such as high T_c superconductivity, colossal magnetoresistance and charge-orbital ordering, take place. The reason is that in these oxides such as MnO, CoO and NiO, transition metal $3d$ electrons are strongly correlated and such strong electron-electron correlations are not adequately treated in LDA or GGA. Therefore, many attempts to go beyond the LDA/GGA approximations have been made in the past few years. Indeed, several rather successful schemes such as self-interaction correction (SIC), optimized effective potential (OEP) and LDA+ U , have been developed.

In Fig. 5, spin-decomposed density of states of cubic Fe_3O_4 from both LDA and LDA+ U calculations are displayed, together with

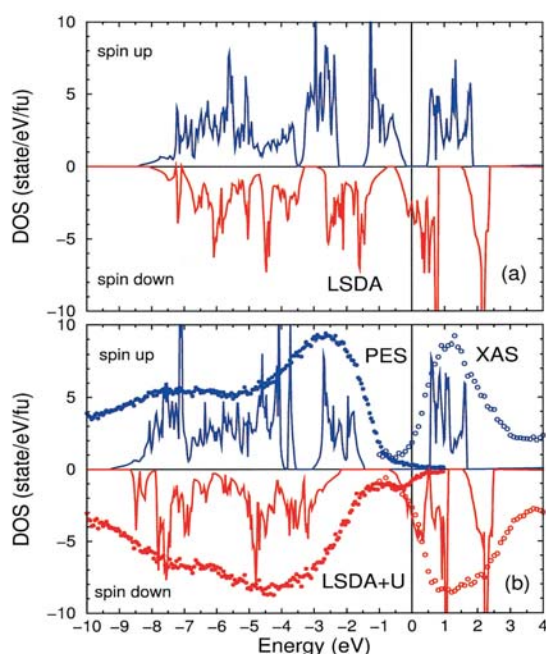


Fig. 5: Spin-decomposed density of states of cubic Fe_3O_4 from LDA calculations (a) and from LDA+ U calculations (solid lines) (b), compared with spin-resolved photoemission spectra (PES) and spin-resolved O K -edge X-ray absorption spectra (XAS) from Fe_3O_4 . The experimental spectra are in arbitrary units and zero energy denotes the Fermi level.

spin-resolved photoemission and O K -edge X-ray absorption spectra. Though Fe_3O_4 is not an archetype of strong correlated electron systems, Figure 5 nonetheless shows that taking on-site Coulomb interaction U into account LDA+ U considerably improves the agreement between the calculated spin-decomposed DOS and the experiments. Furthermore, LDA gives an orbital magnetic moment of B -site Fe ions that is one order of magnitude too small whilst, in contrast, LDA+ U brings both the theoretical orbital and spin magnetic moments in Fe_3O_4 in good agreement with soft X-ray magnetic circular dichroism experiments and also neutron scattering measurements.

Authors:

G. Y. Guo

Department of Physics, National Taiwan University, Taipei, Taiwan

L. S. Hsu

Department of Physics, National Chang-Hua University of Education, Chang-Hua, Taiwan

D. J. Huang

National Synchrotron Radiation Research Center, Hsinchu, Taiwan

H. T. Jeng

Physics Division, National Center for Theoretical Sciences, Hsinchu, Taiwan

Publications:

- L.-S. Hsu, G. Y. Guo, J. D. Denlinger, and J. W. Allen, Phys. Rev. B **63**, 155105 (2001).
- G. Y. Guo, Y. K. Wang, and L.-S. Hsu, Phys. Rev. B **66**, 54440 (2002).
- H.-T. Jeng, D. J. Huang, G. Y. Guo, and J. Chen, Phys. Rev. B (submitted).

Contact e-mail:

gyguo@phys.ntu.edu.tw